



Research paper

Effective connectivity between resting-state networks in depression

Dana DeMaster^{a,*,1,2}, Beata R. Godlewska^{b,c,1}, Mingrui Liang^d, Marina Vannucci^d,
Taya Bockmann^e, Bo Cao^f, Sudhakar Selvaraj^e

^a Children's Learning Institute, Department of Pediatrics, University of Texas Health Science Center at Houston, McGovern Medical School, Houston, TX, USA

^b Department of Psychiatry, Medical Sciences Division, University of Oxford, United Kingdom.

^c Oxford Health NHS Foundation Trust, Oxford, United Kingdom

^d Department of Statistics, Rice University, Houston, TX, USA.

^e Department of Psychiatry and Behavioral Sciences, University of Texas Health Science Center at Houston, McGovern Medical School, Houston, TX, USA.

^f University of Alberta, Department of Psychiatry, Edmonton, Canada.

ARTICLE INFO

Keywords:

Depression

Resting state fMRI

Effective connectivity

Escitalopram

Treatment response

ABSTRACT

Rationale: Although depression has been widely researched, findings characterizing how brain regions influence each other remains scarce, yet this is critical for research on antidepressant treatments and individual responses to particular treatments.

Objectives: To identify pre-treatment resting state effective connectivity (rsEC) patterns in patients with major depressive disorder (MDD) and explore their relationship with treatment response.

Methods: Thirty-four drug-free MDD patients had an MRI scan and were subsequently treated for 6 weeks with an SSRI escitalopram 10 mg daily; the response was defined as $\geq 50\%$ decrease in Hamilton Depression Rating Scale (HAM-D) score.

Results: rsEC networks in default mode, central executive, and salience networks were identified for patients with depression. Exploratory analyses indicated higher connectivity strength related to baseline depression severity and response to treatment.

Conclusions: Preliminary analyses revealed widespread dysfunction of rsEC in depression. Functional rsEC may be useful as a predictive tool for antidepressant treatment response. A primary limitation of the current study was the small size; however, the group was carefully chosen, well-characterized, and included only medication-free patients. Further research in large samples of placebo-controlled studies would be required to confirm the results.

1. Introduction

Major depressive disorder (MDD) is a common and debilitating mental illness worldwide (Whiteford et al., 2013). Therefore, a better understanding of underlying biological mechanisms is crucial for better clinical management and treatment development. The importance of this is evident given restrictions of current antidepressant treatments: they are chosen on a trial and error basis, achieving clinically significant response takes a few weeks at best and nearly 30% of depressed patients

do not respond to treatment even after multiple trials (McIntyre et al., 2014; Warden et al., 2007).

The human brain is considered a dynamic and complex interconnected network of brain regions termed intrinsic connectivity networks (ICNs) (Pessoa, 2014). Currently, MDD is instead univocally accepted to be a brain network disorder, in which the problem is a malfunction and disturbed communication of many structures, rather than dysfunction of one particular brain region (Li et al., 2018). Characterizing brain circuitry involved in MDD and understanding how

Abbreviations: ACC, Anterior cingulate cortex; CEN, Central executive network; DMN, Default mode network; dlPFC, Dorsolateral prefrontal cortex; dmPFC, Dorsomedial PFC; EC, Effective Connectivity; FPN, Frontoparietal network; IFG, Inferior frontal gyrus; ICNs, Intrinsic connectivity networks; MDD, Major depressive disorder; MTL, Middle temporal lobe subsystem; mOFC, Orbito-frontal cortex; PCC, Posterior cingulate cortex; SN, Salience network; vlPFC, Ventrolateral PFC.

* Corresponding author at: Department of Pediatrics, Children's Learning Institute, University of Texas Health Science Center at Houston, McGovern Medical School, Houston, TX, USA.

E-mail address: Dana.M.demaster@uth.tmc.edu (D. DeMaster).

¹ Contributed equally.

² Add: 6655 Travis Ste. 1015, Houston, Texas, 77,030

<https://doi.org/10.1016/j.jad.2022.03.041>

Received 1 October 2021; Received in revised form 12 March 2022; Accepted 17 March 2022

Available online 21 March 2022

0165-0327/© 2022 The Authors. Published by Elsevier B.V. This is an open access article under the CC BY-NC license (<http://creativecommons.org/licenses/by-nc/4.0/>).

current treatments affect the brain is critical in developing novel treatment opportunities.

Evaluated with functional magnetic resonance imaging (fMRI), disrupted functional connectivity in the brain involving several core brain ICNs has been consistently associated with altered connectivity in patients with MDD. The core networks implicated in MDD include the default mode network (DMN), the central executive network (CEN) and the salience network (SN) (Andrews-Hanna et al., 2014; Brakowski et al., 2017; Kaiser et al., 2015; Mulders et al., 2015). The ICN, that is most consistently shown as disturbed in depression, is the DMN, which plays a role in self-referential processing (Andrews-Hanna et al., 2014; Greicius et al., 2009; Vincent et al., 2006). The DMN consists of at least three subsystems, the anterior DMN (aDMN), with the hub in the medial prefrontal cortex (mPFC, in particular pregenual anterior cingulate cortex, pgACC), posterior DMN (pDMN), with the main hubs being the precuneus and inferior and posterior cingulate cortex (PCC), and the middle temporal lobe subsystem (MTL), including structures such as middle temporal gyrus, hippocampus and parahippocampal cortex (Andrews-Hanna et al., 2010; Buckner et al., 2008; Moussa et al., 2012). The CEN is associated with working memory and control processes and consists of the bilateral dorsolateral prefrontal cortex (dlPFC), ventrolateral PFC (vlPFC), dorsomedial PFC (dmPFC), lateral parietal cortices and left fronto-insular cortex (Marek and Dosenbach, 2018, 2019; Seeley, 2019). The SN main hubs include anterior insula and dorsal ACC (dACC) that control the switch between the CEN and DMN and impacts how a stimulus is processed (Menon, 2019; Moussa et al., 2012).

The most commonly used approach for identifying differences in ICNs in depressed individuals is resting-state functional connectivity (rsFC), which captures temporally correlated brain functioning within the ICNs. RsfMRI identifies temporally correlated regions at rest (Seeley et al., 2007) and is acquired in the absence of any particular task or stimulus (Smitha et al., 2017). RsfMRI studies showed widespread network-level connectivity alterations (Kaiser et al., 2015) and treatment response-related changes in depression (Dichter et al., 2015). Meta-analyses supported the importance of dysfunction within and between the DMN and CEN in MDD. For example, a meta-analysis of 25 rsFC studies (Kaiser et al., 2015), showed increased connectivity both within the frontoparietal network (FPN, equivalent to CEN) and the DMN. The authors observed a decrease in rsFC between FPN and DMN regions and increased connectivity between the DMN and the left dlPFC. Reduced connectivity was also observed between areas of the affective network (which is part of the SN) and the mPFC, a part of the DMN. Connectivity between the ventral attention network (part of the SN) and FPN and DMN seemed generally altered, while connectivity between DMN and thalamus and putamen was decreased (Kaiser et al., 2015). Brakowski et al. (Brakowski et al., 2017) conducted a meta-analysis of 94 studies and found altered connectivity in depressed subjects associated with several MDD symptoms. Rumination seemed connected to decreased connectivity between the anterior and posterior DMN (Zhu et al., 2012). The severity of symptoms in depressed patients seems to correlate with altered functional connectivity within the right anterior insula and the anterior DMN (Coutinho et al., 2016; Manoliu et al., 2013).

One of the major limitations of FC approaches is that time-dependent causal relationships between regions cannot be inferred. On the other hand, Effective Connectivity (EC) offers an alternative approach to explicitly measure *directionality*, or the influence of one region on another in time. EC is a useful approach for characterizing the influence of the activity of region A on subsequent activity in region B which is a key prerequisite for inferring causal direction within a brain network. From this perspective, a major strength of EC is that temporal primacy provides specific information about dependency among brain regions from which the attributes of disrupted ICNs in depression are inferred (Friston, 2011). The statistical approach used to model EC for the current research is appropriate for patient populations across large age ranges (Kook et al., 2021).

The primary objective of this study was to investigate the *resting-state effective* (i.e., *directed*) connectivity between different brain regions and networks using a *non-biased data-driven approach* in patients with MDD undergoing antidepressant treatment. Analyses targeted connectivity of DMN, CEN, and SN because aberrant functioning of these three neuro-cognitive networks is evident across multiple disorders (Menon, 2011), including MDD (Zheng et al., 2015; Brakowski et al., 2017). Additionally, we explored a relationship between effective connectivity strength and response to 6-weeks treatment with escitalopram, and evaluate effect of depression severity on that relationship. These exploratory analyses are an initial step towards a mechanistic understanding of neurobiological systems that underlie individual differences affecting response to treatment.

2. Methods

2.1. Participants and study design

The study was approved by the Oxford Research Ethics Committee and performed in accordance with Declaration of Helsinki.

Patients with MDD were recruited into the study by advertising in local newspapers and through referrals from clinicians. In total, written informed consent to participate in the study was obtained from 39 patients with MDD (24F:15M). All MDD patients had a response to treatment assessed after six weeks of treatment.

All participants were assessed with the Structured Clinical Interview for DSM-IV (First, 1997) to present current and past psychiatric disorders. Depressed patients met DSM-IV criteria for a primary diagnosis of major depressive disorder; exclusion criteria for both groups were: past/current DSM-IV diagnosis of axis I disorder (other than MDD inpatient group), substance dependence as defined by DSM-IV, a clinically significant risk of suicidal behavior, major somatic or neurological disorders, pregnancy or breast-feeding, any contra-indications to MR imaging, or concurrent medication that could alter emotional processing. In addition, patients with contraindications to escitalopram treatment or treatment with psychotropic medication less than three weeks before the study (5 weeks for fluoxetine) were also excluded. All participants were right-handed.

After the baseline fMRI scan, patients received 10 mg escitalopram each morning for six weeks without dose adjustment. Depression severity was measured using the 17-item Hamilton Depression Rating Scale (HAMD) (Hamilton, 1960) and Beck Depression Inventory (BDI) (Beck et al., 1961), at baseline and after six weeks of treatment. After completion of the study, patients were offered treatment openly with escitalopram according to usual clinical practice. Clinical response to the selective serotonin reuptake inhibitor (SSRI) was defined as a reduction in HAMD of 50% or more from baseline after six weeks of treatment (Angst et al., 1993).

The current analysis focuses on baseline differences in *effective* rsFC. This research is a part of a larger study, in which medication-free patients with depression were treated with 10 mg escitalopram for 6 weeks without dose adjustment (for published task fMRI papers see (Godlewska et al., 2018; Godlewska et al., 2012).

2.2. Data acquisition

Resting-state data acquisition was performed with participants having their eyes closed. fMRI data were acquired on a 3T Siemens Magnetom TIM TRIO scanner (Siemens AG) at the University of Oxford Centre for Clinical Magnetic Resonance Research (OCMR). A total of 180 volumes of resting-state fMRI (rs-fMRI) were acquired with a voxel resolution of $3 \times 3 \times 3.5$ mm, repetition time (TR)/echo time (TE)/flip angle (FA) = 2000 ms/28 ms/89°. T1-weighted structural images were acquired using a magnetization prepared rapid acquisition by gradient echo sequence (MPRAGE) with a voxel resolution $1.0 \times 1.0 \times 1.0$ mm on a $208 \times 256 \times 200$ grid, TR/TE/inversion time (TI) = 2040 ms/4.68 ms/

900 ms. Gradient echo phase and magnitude field maps to correct for distortion were also acquired with a voxel resolution of $3.5 \times 3.5 \times 3.0$ mm, TR/TE1/TE2/FA = 488 ms/5.19 ms/7.65 ms/60°. The fMRI session was completed in 60–90 min.

2.3. Image processing

Standard preprocessing steps in FreeSurfer's (VERSION 5.3; <http://surfer.nmr.mgh.harvard.edu>) recon-all pipeline were applied to each subject's T1 as part of automated segmentation of cortical and subcortical brain into aparc+aseg anatomical regions (Dale et al., 1999; Lindemer et al., 2013). These steps resulted in 110 distinct ROIs (Supplementary Table 1). ROI's corresponding to grey matter were used as seed regions in subsequent rsfMRI analyses, excluding ventricles and white matter. fMRI acquisitions were processed following standard procedures in the FreeSurfer Functional Analysis Stream (FSFAST) processing stream (<http://freesurfer.net/fswiki/FsFast>), including motion correction, time-shifting, concatenation of scans, motion regressed out of time series, and band pass filtering between 0.01 and 0.1 Hz. We applied spatial smoothing with a Gaussian kernel of full-width at half maximum of 6 mm and temporal filtering with a high-pass filter cut-off of 150 s (0.007 Hz). Correction parameters were included as nuisance regressors following standard FSFAST procedure. Participants with excessive motion (.2 mm) on more than 15% of time points were excluded from further analyses. Region-of-interest (ROI) analyses were performed using AFNI (<https://afni.nimh.nih.gov/>), resulting in the time-series corresponding to each FreeSurfer aparc+aseg anatomical regions. Time series were then standardized via z-score transformation prior to statistical analysis.

2.4. Statistical analysis

All statistics related to group characteristics were performed in R Core Team. Chi-square and independent, two-sample *t*-tests and Mann-Whitney tests were used to test for demographic differences between groups. Mann-Whitney tests were used instead of independent two-sample *t*-tests if the measures were not normally distributed.

Broadly, a data driven approach was used for first level of analysis, which estimated region to region connections globally. To characterize connectivity between regions, we fitted the time series data using a Bayesian multi-subject vector autoregressive (VAR) model (Chiang et al., 2017). This modeling framework uses a Bayesian variable selection approach to allow for simultaneous inference on effective connectivity at both the subject and group levels. The requisite detailed steps followed in our implementation of BVAR-connect were recently published (Kook et al., 2021), a Matlab software available for download at <https://github.com/marinavannucci> and at <https://github.com/rimehi>. Briefly, this software uses an approximation method for statistical inference known as variational Bayes to allow for scalable inference on a whole-brain at an efficient computational cost. For model fitting, the default parameter setting provided in BVAR-connect was used. The inferred effective connectivities and resultant connectivity strengths were then exported to Excel CSV files for further analysis and visualizations. In this application of BVAR-connect, group level effective connectivity estimation was conducted for the sample as a whole, without group level comparison (i.e., no comparison of responders and non-responders). Specifically, connectivity dynamics were estimated globally such that for our sample connections and connectivity strengths were indexed for every brain region to every other brain region across one group. The model was fit using the 'model fitting' interface of the user-friendly BVAR-connect Matlab GUI. Default values for all the model parameters were used, as provided by the software. The method identified nonzero effective connectivities by thresholding posterior probabilities of nonzero edges at a pre-specified threshold of 0.5. Connectivity strength values were then calculated as estimates of the coefficients of the autoregressive model (i.e., BVAR). For region to region connections

identified at the group level, BVAR-connect simultaneously estimate connectivity strength at the subject level.

Connectivity strength at the subject level was used in exploratory analyses discussed in the following section. Connectivity strength at the subject level was used in exploratory analyses discussed in the following section.

All statistics for exploratory analyses were performed in IBM SPSS Statistics. The effects of depression severity and response to medication on region-to-region effective connectivity at rest were examined with a series of General Linear Models (GLMs). These analyses were restricted to region-to-region connections identified in group-level analyses for DMN, CEN, and SN (DMN, CEN, and SN region assignment is listed in Fig. 1; Supplementary Table 1 provides a comprehensive list of region network assignment). Connectivity strength was included as the dependent variable with depression severity, timepoint, and response as independent variables and age included as a covariate. The model tested a 2-way interaction (depression severity X response to intervention). Owing to the exploratory nature of this analysis, we provide statistics (F and Cohen's d) for all models meeting the significance threshold that was set at $p < 0.05$; however, model significance was also evaluated using Bonferroni corrected *p*-values (0.05/number of connections evaluated for each network) as noted in Table 2. This exploratory analysis approach, GLM evaluating relationships between psychological health outcomes and DMN effective connectivity strength resulting from group level BVAR-connect analyses, was previously applied to fMRI data from children with history of pediatric head injury (see Vaughn et al., 2022).

3. Results

Both baseline fMRI data and data on response to six weeks treatment with escitalopram were available for 34 patients (four patients dropped out before the 6-week assessment, scanning data from one patient were unavailable due to excessive motion). After six weeks of treatment with escitalopram, 21 (62%) patients were classified as responders. Responders and non-responders did not differ with respect to gender, age, baseline depression severity, age at depression onset and duration of the current episode (see Table 1 for details).

3.1. Effective connectivity

A total of 50 connections were evident between regions assigned to DMN, CEN, and SN. Within network and between network connections are discussed below.

There were 15 positive connections detected between regions in the DMN (Fig. 1A, Left). Effective connectivity, localized to posterior DMN, included: connectivity between left and right isthmus (cingulate) which was evident with bilateral origin and termination points (i.e., from left to right and vice versa); right precuneus to left precuneus; and right precuneus to right isthmus. DMN effective connectivity that was more anterior originated from left rostral ACC connecting to right rostral ACC. Left rostral ACC also connected to posterior DMN by way of left isthmus and left PCC. Right middle temporal connected to left middle temporal and bilaterally to inferior parietal. Right superior temporal connected to left superior temporal, left precuneus and right hippocampus. Effective connectivity from left to right was evident between hippocampi.

Effective connectivity originating from DMN connecting to CEN (2 connections) and DMN connecting to SN (3 connections) is presented in Fig. 1A, Right. DMN connected to CEN originating in left rostral ACC to superior frontal cortex bilaterally. DMN connected to SN originating in left rostral ACC connecting to caudal ACC (bilaterally) and with connectivity originating in left inferior parietal (DMN) connecting to left insula (SN).

Within CEN effective connectivity was evident in 15 connections primarily originated in and connected to regions within VLPFC (Fig. 1B, Left). Specifically, seven *intra*-VLPFC connections were evident, all within hemisphere except for right pars triangularis connecting to left

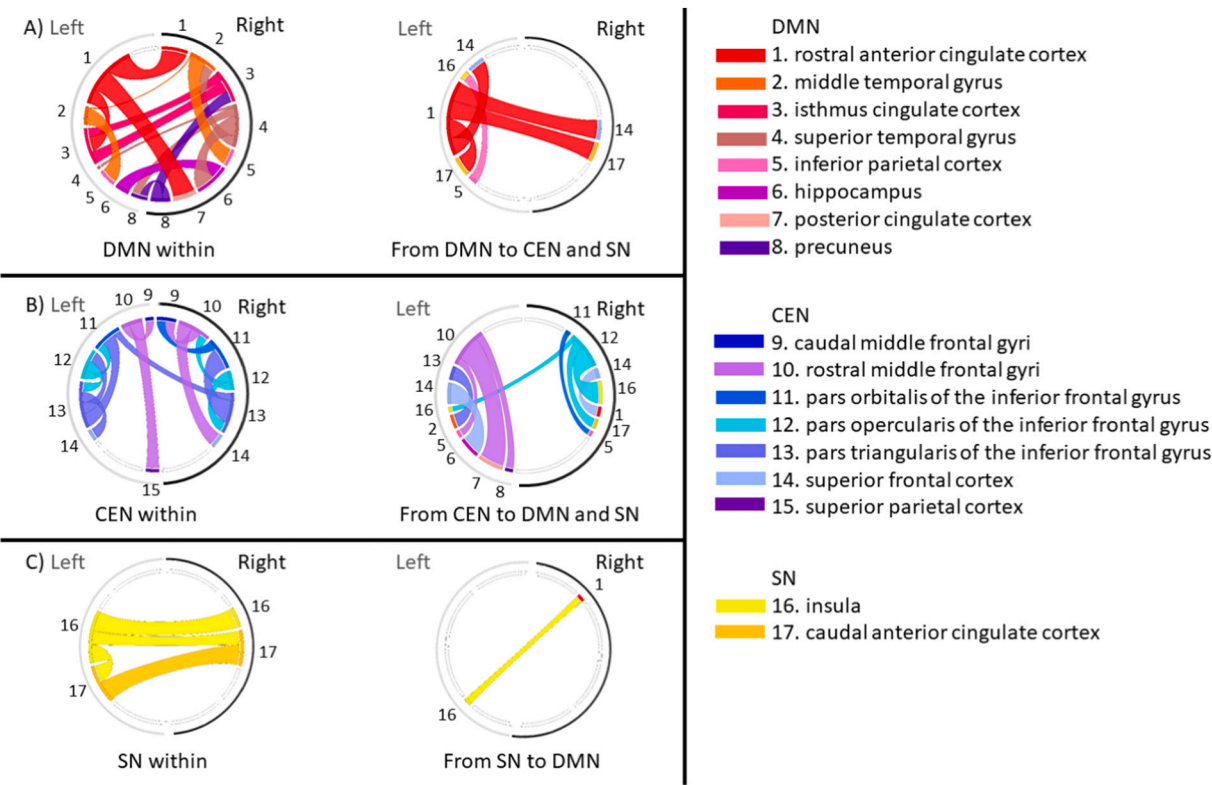


Fig. 1. Connectograms showing rsEC within network connectivity (A) Default Mode Network, (B) Central Executive Network, and (C) Salience Network. Connectivity within each network is on the left and network connectivity between each network and other two networks is on the right. The width of each line indicates connectivity strength, with a wider line representing stronger connections. Temporal primacy is indicated by lines connected to the circle with the same color. The outside circle indicates left hemisphere connections in grey and right hemisphere connections in black. The numbers correspond to the numbered regions in the key.

Table 1
Demographics and clinical scores, presented as a mean \pm standard deviation (SD). Treatment responders (R) and non-responders (NR) differed significantly at week 6 in HAM-D score ($t = -8.442, p < 0.0001$) and BDI score ($t = -4.899, p < 0.0001$). All other differences between R and NR were not significant ($p > 0.05$).

	Responders N = 21	Non-responders N = 13
Age (years)	30.4 \pm 11.7	30.1 \pm 10.1
Gender	11F and 10 M	8F and 5 M
Age at onset (years)	25.1 \pm 8.3	25.2 \pm 11.3
Duration of current episode (months)	5.9 \pm 6.1	8.8 \pm 8.7
HAMD baseline	23.3 \pm 4.9	22.9 \pm 4.0
HAMD at 6 weeks	4.5 \pm 3.8	17.4 \pm 5.1
BDI baseline	31.6 \pm 6.8	32.4 \pm 5.5
BDI at 6 weeks	9.2 \pm 7.3	24.2 \pm 10.6

pars orbitalis. VLPFC also connected to middle frontal (Left: pars triangularis to superior frontal and pars triangularis to caudal middle frontal; Right: pars orbitalis to caudal middle frontal and pars opercularis to rostral middle frontal). Rostral middle frontal showed 4 additional within hemisphere connections CEN (i.e., connecting bilaterally to caudal middle frontal and superior parietal). CEN connections to DMN (7 connections) and CEN connections to SN (3 connections) are shown in Fig. 1B, Right. All CEN to DMN connections were within hemisphere. On the left there were three connections originating from CEN (rostral middle frontal) connected to posterior DMN (PCC, inferior parietal cortex, and precuneus). There were two VLPFC connections from CEN to DMN (right pars orbitalis to inferior parietal and left pars triangularis to middle temporal gyrus). Finally, left superior frontal (CEN) connected to hippocampus (DMN) and right superior frontal (CEN) connected to rostral ACC (DMN). CEN connected to

SN via VLPFC (right pars opercularis) connecting to right caudal anterior cingulate (SN) and insula (SN, bilaterally). There were 4 intra-salience network connections identified with all connectivity that originated in the left hemisphere (Fig. 1C, Left). Specifically, left to right connections between insula to itself and ACC itself were identified. Connectivity originating in insula connecting to left and right caudal ACC was also evident. Connectivity that originated in SN extended to DMN was evident in a single connection (i.e., left insula to right rostral anterior cingulate) but not SN to CEN (Fig. 1C Right). Table 2 provides Linear Mixed Models (fixed and random effects) results indicating significant interactions between initial severity and response to intervention (2-way interaction) Note. Cohen's d provide over 0.2 and * indicating significant Bonferroni-corrected p-values. Exploratory analyses were restricted to the 50 DMN, SN and CEN connections that were evident at the group level. For DMN and CEN, significant 2-way interactions indicate that depression severity effective connectivity relations were different between R and NR, although the overall pattern was consistent across timepoints. As demonstrated in Fig. 2, the 2-way interactions showed a pattern of low effective connectivity strength for NR across the initial severity of depression. In contrast, responders with high depression scores showed high connectivity strength and responders with low depression showed low connectivity strength. This pattern of results is evident for most connectivities (see supplemental Table 2). There were two exceptions, right pars orbitalis to right caudal middle frontal (Fig. 2; CEN) and left insula to right rostral anterior cingulate (SN to DMN), where NR with high initial depression shows higher connectivity. Broadly, SN significant 2-way interactions indicate that depression severity effective connectivity relations were different between R and NR with NR showing more pronounced severity effects relative to R. Whereas DMN and CEN connectivity was consistent across time, SN connections with significant 2-way interactions showed main effect of timepoint characterized by

Table 2

Relationship between effective connectivity, depression severity, and outcome.

Region						
Origin (from)	Termination (to)	Age F	Severity F d	Timepoint F d	Response F d	Response X Severity F d
Network: Within DMN						
L Hippocampus	R Hippocampus	14.19	0.005	0.31	1.23	9.61 d = 0.64
R middle temp.	R inferior parietal	7.81	0.29	1.53 d = −0.37	0.21	9.04 d = −0.34
L middle temp.	L inferior parietal	2.68	3.41 d = −0.61	0.42	0.03	6.81 d = 0.26
Network: Within CEN						
R pars orbitalis	R caud mid. front	3.67	1.04 d = −0.26	0.37	0.01	9.51 d = 0.39
Network: Within SN						
L Insula	R cuad. ant. cing	3.64	0.10	5.08 * d = 0.39	2.30 d = −0.37	5.83 d = −0.65
Network: From CEN to DMN						
R pars orbitalis	R inferior parietal	0.43	3.61 d = −0.63	1.33 d = 0.37	2.75 d = 0.63	7.07* d = 0.39
Network: From CEN to SN						
R pars opercula.	R insula	6.46	0.01	1.61	4.63 d = 0.75	6.75* d = −0.24
Network: From SN to DMN						
L Insula	R rost. ant. cing	0.18	3.53 d = −0.52	3.48* d = 0.50	0.95 d = −0.23	11.03* d = −0.39

increase in connectivity over time.

4. Discussion

The preliminary analysis identified resting-state effective connectivity (rsEC) networks for patients with depression and explore differences in connectivity related to depression severity and response to treatment. The most striking general feature, illustrated in Fig. 1, was rsEC observed in DMN, CEN and SN areas in MDD patients, indicating robust DMN/CEN connectivity but limited and low strength connection from SN to DMN and no connection to CEN. Consistent with previous literature, this finding adds to a growing awareness that weak connectivity from SN to DMN/CEN might be mechanistically linked to affective disorder through disruption to SN modulated physiological reactivity to salient stimuli and diminished inability to cycle out of internal mental processes to attend to salient task-relevant external stimuli (Menon, 2011; Zheng et al., 2015; Brakowski et al., 2017). Following network connectivity estimation, additional analyses were performed to explore whether connections were involved in response to antidepressant escitalopram and to assess the impact of initial depression severity. We also showed that an association of higher connectivity strength with treatment response depended on baseline depression severity, classified as mild-moderate or severe on the basis of the baseline HAM-D score.

Changes in rsEC in the MDD group were present within and between the ICNs whose dysfunction has been consistently reported in MDD, the DMN, the CEN and the SN (Kaiser et al., 2015; Zhong et al., 2016). These networks remain in a close relationship and their harmonious communication is crucial for healthy mental function. DMN's activity is the highest during inward-directed processing in the healthy brain, such as self-referential processing, imagery and memory (Buckner et al., 2008). With some exceptions, it decreases when resources are required for external attention-demanding tasks; this is when the CEN becomes most active (Wang et al., 2012). The SN facilitates the switch (Menon, 2019). Increased activity of the DMN, with an inability to switch off when

necessary, has been one of the most consistent findings in depression research, and is suggested to underlie negative ruminations typical for depression (Dutta et al., 2014). While increased temporal coherence of the activity of DMN's regions has been frequently reported, an assessment of the direction of the effect has been less commonly performed. Our MDD group was characterized by increased rsEC from the anterior to posterior DMN (from the left rACC to the left isthmus of the cingulate/left PCC). At the same time, no increase in connectivity strength was noticed in the reverse direction, suggesting the dominance of the anterior over posterior DMN. Although we did not assess ruminations in our study, increasing connectivity from the rACC to PCC has been proposed as the neural basis of ruminations. Thereby suggesting that dysfunctional communication from the aDMN to pDMN may be relevant to developing and maintaining at least some symptoms of depression (Brakowski et al., 2017). In the MDD group, the connectivity strength was highly increased between the structures of the pDMN – the precuneus, the PCC and the isthmus of the cingulate, and the pDMN to the hippocampus. The DMN subnetworks, apart from sharing general DMN roles, have specific functions (Buckner et al., 2008). The aDMN is biased towards self-other relations, while the pDMN shows a greater bias towards self-centred processing and plays a role in involuntary (bottom-up) attentional processing (Buckner et al., 2008). Increased strength of connections within the pDMN, and between the pDMN and the hippocampus may promote the bias towards inward-directed versus self-other processing, supporting retrieval of negative-valenced memory traces. The pDMN has been previously suggested to play a particular role in antidepressant response (Li et al., 2013; Posner et al., 2013; Shen et al., 2015; Wang et al., 2012).

The DMN's function depends not only on the communication between its structures but also on communication with other networks, particularly the CEN (Marek and Dosenbach, 2018, 2019). The CEN is involved in higher-order cognitive processing and executes control in response to salient input (Seeley et al., 2007). In the healthy brain, when resources are needed for goal-directed behavior, the balance of activity

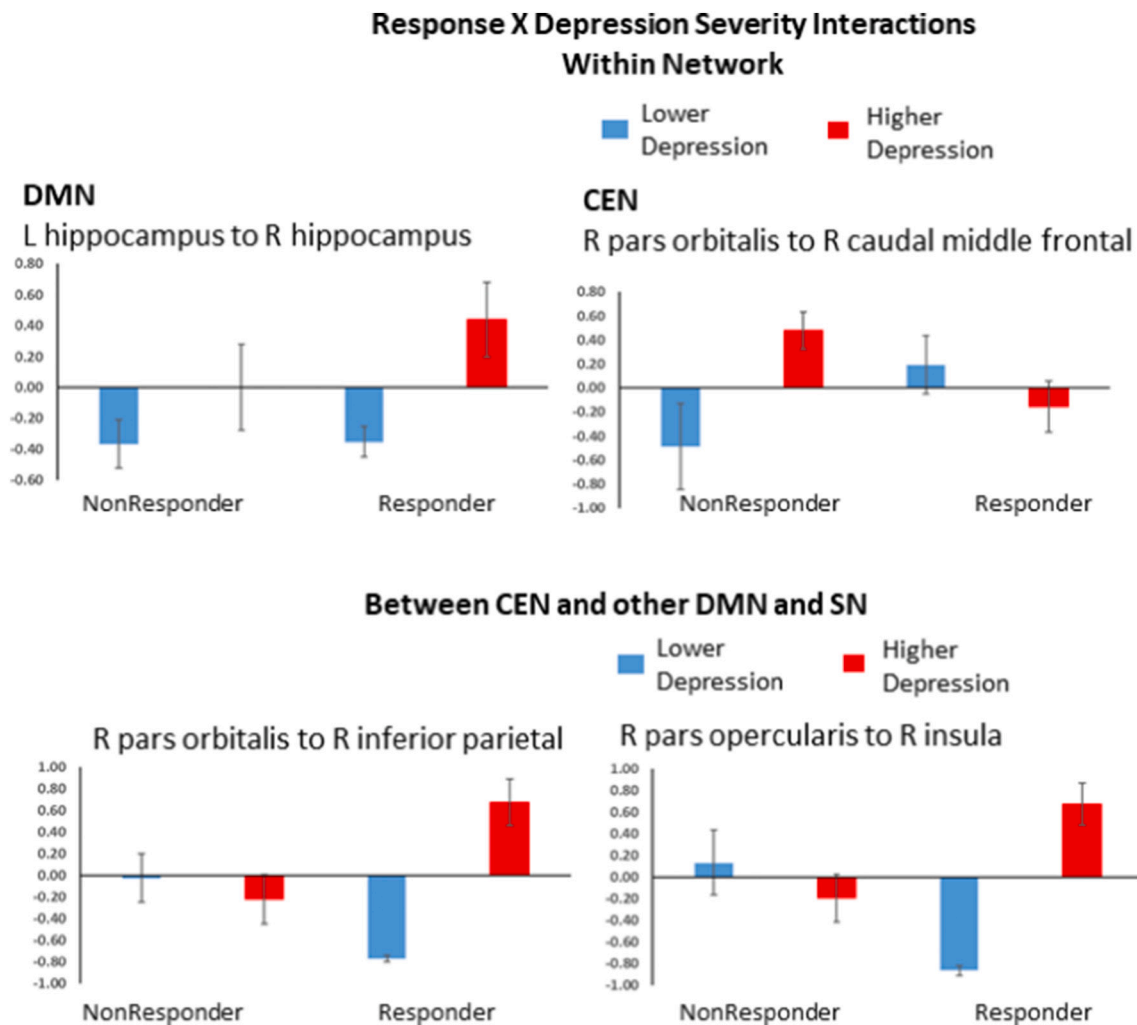


Fig. 2. Showing effective connectivity strength for left Hippocampus to right Hippocampus (DMN), right pars orbitalis to right Caudal middle frontal (CEN), right pars orbitalis to right inferior parietal (CEN to DMN) and right pars opercularis to right insula (CEN to SN). Non-responder (NR) group is on the left and responder group is on the right with enrolment HAMD less than 23 (Lower Depression) in blue and enrolment HAMD of 23 or above (Higher Depression) in red. *Effective connectivity strength reflects z-score adjusted for age such that zero reflects average effective connectivity strength. (For interpretation of the references to color in this figure legend, the reader is referred to the web version of this article.)

shifts in favor of the CEN, over the DMN (Shaw et al., 2021). In our MDD group, we observed strongly increased rsEC within the CEN (between the parts of the IFG, mostly within the same hemisphere) and from the CEN to pDMN (left rMFG to PCC). Several connections showed modestly increased connectivity strength: from the aDMN to CEN (left rACC to left and right SFG), from the CEN to aDMN (right SFG to right rACC), and from the CEN to MTL (pars triangularis of the left IFG to left MTG). Speculatively, an increase in connectivity strength, particularly within the CEN, and from the CEN to DMN, maybe a compensatory attempt for the significant increase in the strength of connections within the DMN. Such findings have been previously reported in task based fMRI studies (Harvey et al., 2005). Given the disproportionally large increase in connectivity strength within the DMN, such compensatory efforts might be insufficient.

Increased rsEC was also present in the SN, the network crucial for executing the switch between the DMN and CEN and redirecting attentional resources appropriately to the environmental requirements (Menon, 2019; Seeley, 2019). We observed rsEC from the part of the CEN, the pars opercularis of the right IFG, to the key region for the switch, the anterior insula (Menon, 2019), particularly strong to the right insula. Increased rsEC in MDD patients was also seen within the SN, from the left insula to bilateral dACC, and from the left to right dACC. At

the same time, we did not see changes in the connectivity between the SN and DMN. Increased strength of connectivity from the CEN to SN, in particular to the right insula, might reflect an attempt of the CEN to execute control over the DMN. However, it is possible that CEN's inhibitory influence on DMN might fail due to poor connectivity from the SN to DMN and translate into inefficient switching between the DMN and the CEN.

To summarize, we showed widespread dysfunction of rsEC in depression. It involved alterations in rsEC within and between the DMN, CEN, and SN, whose harmonious collaboration is necessary to balance internally- and externally-oriented processing and an appropriate and flexible resource allocation. We also showed changes in rsEC between the areas involved in reward processing and both the DMN and CEN, which supports models suggesting the central role of reward processing in depression. As a general rule, the DMN to CEN connections were strong, while connections from the CEN to DMN, although more numerous, were weaker, possibly translating into weakened control of the DMN and relative DMN dominance.

Additionally, we explored the relationship between connectivity strength and response as a function of initial depression severity, defined as mild-moderate and severe based on HAMD score. Across many connections, the pattern was similar – such that responders with low and

high depression scores showed a significant differences in connectivity strength; whereas, NR not differing in this regard, regardless of depression severity, with connectivity strength intermediate in respect to responders. Heterogeneity in MDD is not well understood; however, investigating correspondence between diagnostic classifiers, such as depression severity, and neurobiological systems will shift the field closer to a mechanistic understanding treatment response. By enlarge exploratory analysis results indicated depression severity by response to treatment effects for region to region connectivity aligned to networks that are noted to underlie top-down attentional control processes. A recent review reported that disrupted attention often but not always accompanies MDD (Keller et al., 2019). Findings of exploratory analyses might contribute to this burgeoning research domain by highlighting the role of attention in differentiated response to depression treatment. As an example, in identifying the direction of EC from inferior frontal gyrus to the insula, we can infer function underlying controlled attentional switching. Our exploratory analyses indicate rsEC for inferior frontal gyrus to the insula differs between responders and non-responders such that for responders rsEC increases with depression severity. One possibility is that increased connectivity between these regions underlies the capacity to re-orient attention away from salient negative valenced thoughts or information to goal relevant information (Keller et al., 2019). Ultimately, findings suggest that the baseline depression severity may be a factor that needs to be considered when looking into employing EC as a tool for response prediction. Unfortunately, no previous resting state explored this subject, and due to the small number of patients, this interesting results warrant careful interpretation.

5. Strengths and limitations

The main strength of the current study was the use of effective connectivity analysis, performed globally, i.e. assessing a relationship of each region in the brain with every other brain region. Using a network model of causal dynamics, effective connectivity offers a unique opportunity to explore the directionality and strength of functional connections in the brain. For this reason, it allows an assessment of causality, i.e. which brain region influences another. Using this method, we were able to explore altered communication of the brain regions in depression and assess the direction of the impact (Friston, 2011). For example, in identifying primacy of functioning in inferior frontal regions relative to insular cortex, we are able to infer causality of the region to region connection which suggests attention allocation as a factor predicting response to treatment. By allowing better mechanistic interpretability, EC has an advantage over functional connectivity analysis, which is a statistical assessment of the synchronicity of function of brain regions in the absence of directionality. Ultimately, the global approach used here allowed us to approach the data without prior assumptions and perform an unbiased assessment of the impact of one structure over another. In addition to estimating effective connectivity networks, this research also implemented the non-biased data-driven methodology. Confirmatory data analysis frameworks that rest on a priori hypotheses tested under structured decision rules lack the analytic flexibility required to detect a difference or change in the brain at a network level. Instead, this investigation utilized the Bayesian multi-subject vector autoregressive (BVAR-connect) approach (Kook et al., 2021), which provided a framework for network identification that maintained analytic flexibility in the absence of external assumptions of network composition.

The main limitation of the current study was the small size of the group, which is linked to power reduction and the likelihood of type 2 error. In particular, a restricted number of good quality datasets were available for an assessment of treatment response. However, the group was carefully chosen, well-characterized, and included only medication-free patients, which allowed a high level of homogeneity. Another limitation was the use of one medication only, escitalopram. Although this increased homogeneity of the procedures, it also means that the

results cannot be generalized to other drugs.

Supplementary data to this article can be found online at <https://doi.org/10.1016/j.jad.2022.03.041>.

Acknowledgements

This work was supported by an MRC program grant (MR/K022202/1) and the Oxford Health NIHR Biomedical Research Centre. The views expressed are those of the authors and not necessarily those of the National Health Service, NIHR or the Department of Health. SS has received grants/research support from NIMH R21 (1R21MH119441 – 01A1) and SAMHSA (FG000470-01). Research supplement funds from The University of Texas Health Science Center at Houston to SS were utilized for this study. The University of Texas Health Science Center at Houston had no role in the design and conduct of the study; collection, management, analysis, and interpretation of the data; preparation, review, or approval of the manuscript; and decision to submit the manuscript for publication. The content of this study is solely the responsibility of the authors and does not necessarily represent the official views of the NIH or SAMHSA.

We thank all the participants for their help with the study.

Conflict of Interest

In the last three years, SS has received speaking honoraria from Global Medical Education, British Medical Journal Publishing Group; own shares at Flow Med Tech. SS received research support from Compass pathways, Janssen and LivaNova.

Dana DeMaster and Beata Godlewska, along with all other authors had no conflicting interests during the last three years.

References

- Andrews-Hanna, J.R., Reidler, J.S., Sepulcre, J., Poulin, R., Buckner, R.L., 2010. Functional-anatomic fractionation of the brain's default network. *Neuron* 65 (4), 550–562. <https://doi.org/10.1016/j.neuron.2010.02.005>.
- Andrews-Hanna, J.R., Smallwood, J., Spreng, R.N., 2014. The default network and self-generated thought: component processes, dynamic control, and clinical relevance. *Ann. N. Y. Acad. Sci.* 1316 (1), 29–52. <https://doi.org/10.1111/nyas.12360>.
- Angst, J., Delini-Stula, A., Stabl, M., Stassen, H.H., 1993. Is a Cut-off Score a Suitable Measure of Treatment Outcome in Short-term Trials in Depression? A Methodological Meta-analysis. <https://doi.org/10.1002/hup.470080503>.
- Beck, A.T., Ward, C.H., Mendelson, M., Mock, J., Erbaugh, J., 1961. An inventory for measuring depression. *Arch. Gen. Psychiatry* 4, 561–571. <https://doi.org/10.1001/archpsyc.1961.01710120031004>.
- Brakowski, J., Spinelli, S., Dörig, N., Bosch, O.G., Manoliu, A., Holtforth, M.G., Seifritz, E., 2017. Resting state brain network function in major depression - depression symptomatology, antidepressant treatment effects, future research. *J. Psychiatr. Res.* 92, 147–159. <https://doi.org/10.1016/j.jpsychires.2017.04.007>.
- Buckner, R.L., Andrews-Hanna, J.R., Schacter, D.L., 2008. The brain's default network: anatomy, function, and relevance to disease. *Ann. N. Y. Acad. Sci.* 1124, 1–38. <https://doi.org/10.1196/annals.1440.011>.
- Chiang, S., Guindani, M., Yeh, H.J., Haneef, Z., Stern, J.M., Vannucci, M., 2017. Bayesian vector autoregressive model for multi-subject effective connectivity inference using multi-modal neuroimaging data. *Hum. Brain Mapp.* 38 (3), 1311–1332. <https://doi.org/10.1002/hbm.23456>.
- Coutinho, J.F., Fernandes, S.V., Soares, J.M., Maia, L., Gonçalves, Ó, F., Sampaio, A., 2016. Default mode network dissociation in depressive and anxiety states. *Brain Imaging Behav.* 10 (1), 147–157. <https://doi.org/10.1007/s11682-015-9375-7>.
- Dale, A.M., Fischl, B., Sereno, M.I., 1999. Cortical surface-based analysis I. Segmentation and surface reconstruction. *Neuroimage* 9 (2), 179–194. <https://doi.org/10.1006/nimg.1998.0395>.
- Dichter, G.S., Gibbs, D., Smoski, M.J., 2015. A systematic review of relations between resting-state functional-MRI and treatment response in major depressive disorder. *J. Affect. Disord.* 172, 8–17. <https://doi.org/10.1016/j.jad.2014.09.028>.
- Dutta, A., McKie, S., Deakin, J.F., 2014. Resting state networks in major depressive disorder. *Psychiatry Res.* 224 (3), 139–151. <https://doi.org/10.1016/j.psychres.2014.10.003>.
- First, M.B., 1997. Structured Clinical Interview for DSM-IV Axis I Disorders. Biometrics Research Department.
- Friston, K.J., 2011. Functional and effective connectivity: a review. *Brain Connect* 1 (1), 13–36. <https://doi.org/10.1089/brain.2011.0008>.
- Godlewska, B.R., Norbury, R., Selvaraj, S., Cowen, P.J., Harmer, C.J., 2012. Short-term SSRI treatment normalises amygdala hyperactivity in depressed patients. *Psychol. Med.* 42 (12), 2609–2617. <https://doi.org/10.1017/s0033291712000591>.

- Godlewska, B.R., Browning, M., Norbury, R., Igoumenou, A., Cowen, P.J., Harmer, C.J., 2018. Predicting treatment response in depression: the role of anterior cingulate cortex. *Int. J. Neuropsychopharmacol.* 21 (11), 988–996. <https://doi.org/10.1093/ijnp/ppy069>.
- Greicius, M.D., Supekar, K., Menon, V., Dougherty, R.F., 2009. Resting-state functional connectivity reflects structural connectivity in the default mode network. *Cereb. Cortex* 19 (1), 72–78. <https://doi.org/10.1093/cercor/bhn059>.
- Hamilton, M., 1960. A rating scale for depression. *J. Neurol. Neurosurg. Psychiatry* 23 (1), 56.
- Harvey, P.O., Fossati, P., Pochon, J.B., Levy, R., Lebastard, G., Lehericy, S., Dubois, B., 2005. Cognitive control and brain resources in major depression: an fMRI study using the n-back task. *NeuroImage* 26 (3), 860–869. <https://doi.org/10.1016/j.neuroimage.2005.02.048>.
- Kaiser, R.H., Andrews-Hanna, J.R., Wager, T.D., Pizzagalli, D.A., 2015. Large-scale network dysfunction in major depressive disorder: a meta-analysis of resting-state functional connectivity. *JAMA Psychiatry* 72 (6), 603–611. <https://doi.org/10.1001/jamapsychiatry.2015.0071>.
- Keller, A.S., Leikauf, J.E., Holt-Gosselin, B., Staveland, B.R., Williams, L.M., 2019. Paying attention to attention in depression. *Transl. Psychiatry* 9 (1), 279. <https://doi.org/10.1038/s41398-019-0616-1>.
- Kook, J.H., Vaughn, K.A., DeMaster, D.M., Ewing-Cobbs, L., Vannucci, M., 2021. BVAR-connect: a variational bayes approach to multi-subject vector autoregressive models for inference on brain connectivity networks. *Neuroinformatics* 19 (1), 39–56. <https://doi.org/10.1007/s12021-020-09472-w>.
- Li, B., Liu, L., Friston, K.J., Shen, H., Wang, L., Zeng, L.L., Hu, D., 2013. A treatment-resistant default mode subnetwork in major depression. *Biol. Psychiatry* 74 (1), 48–54. <https://doi.org/10.1016/j.biopsych.2012.11.007>.
- Li, B.J., Friston, K., Mody, M., Wang, H.N., Lu, H.B., Hu, D.W., 2018. A brain network model for depression: from symptom understanding to disease intervention. *CNS Neurosci. Ther.* 24 (11), 1004–1019. <https://doi.org/10.1111/cns.12998>.
- Lindemer, E.R., Salat, D.H., Leritz, E.C., McGlinchey, R.E., Milberg, W.P., 2013. Reduced cortical thickness with increased lifetime burden of PTSD in OEF/OIF veterans and the impact of comorbid TBI. *Neuroimage Clin.* 2, 601–611. <https://doi.org/10.1016/j.nicl.2013.04.009>.
- Manoliu, A., Meng, C., Brandl, F., Doll, A., Tahmasian, M., Scherr, M., Sorg, C., 2013. Insular dysfunction within the salience network is associated with severity of symptoms and aberrant inter-network connectivity in major depressive disorder. *Front. Hum. Neurosci.* 7, 930. <https://doi.org/10.3389/fnhum.2013.00930>.
- Marek, S., Dosenbach, N.U.F., 2018. The frontoparietal network: function, electrophysiology, and importance of individual precision mapping. *Dialogues Clin. Neurosci.* 20 (2), 133–140. <https://doi.org/10.31887/DCNS.2018.20.2/smerek>.
- Marek, S., Dosenbach, N.U.F., 2019. Control networks of the frontal lobes. *Handb. Clin. Neurol.* 163, 333–347. <https://doi.org/10.1016/b978-0-12-804281-6.00018-5>.
- McIntyre, R.S., Filteau, M.J., Martin, L., Patry, S., Carvalho, A., Cha, D.S., Miguelez, M., 2014. Treatment-resistant depression: definitions, review of the evidence, and algorithmic approach. *J. Affect. Disord.* 156, 1–7. <https://doi.org/10.1016/j.jad.2013.10.043>.
- Menon, V., 2011. Large-scale brain networks and psychopathology: a unifying triple network model. *Trends Cogn. Sci.* 15 (10), 483–506.
- Menon, B., 2019. Towards a new model of understanding - the triple network, psychopathology and the structure of the mind. *Med. Hypotheses* 133, 109385. <https://doi.org/10.1016/j.mehy.2019.109385>.
- Moussa, M.N., Steen, M.R., Laurienti, P.J., Hayasaka, S., 2012. Consistency of network modules in resting-state fMRI connectome data. *PLoS One* 7 (8), e44428. <https://doi.org/10.1371/journal.pone.0044428>.
- Mulders, P.C., van Eijndhoven, P.F., Schene, A.H., Beckmann, C.F., Tendolkar, I., 2015. Resting-state functional connectivity in major depressive disorder: a review. *Neurosci. Biobehav. Rev.* 56, 330–344. <https://doi.org/10.1016/j.neubiorev.2015.07.014>.
- Pessoa, L., 2014. Understanding brain networks and brain organization. *Phys. Life Rev.* 11 (3), 400–435. <https://doi.org/10.1016/j.plrev.2014.03.005>.
- Posner, J., Hellerstein, D.J., Gat, I., Mechling, A., Klahr, K., Wang, Z., Peterson, B.S., 2013. Antidepressants normalize the default mode network in patients with dysthymia. *JAMA Psychiatry* 70 (4), 373–382. <https://doi.org/10.1001/jamapsychiatry.2013.455>.
- Seeley, W.W., 2019. The salience network: a neural system for perceiving and responding to homeostatic demands. *J. Neurosci.* 39 (50), 9878–9882. <https://doi.org/10.1523/jneurosci.1138-17.2019>.
- Seeley, W.W., Menon, V., Schatzberg, A.F., Keller, J., Glover, G.H., Kenna, H., Greicius, M.D., 2007. Dissociable intrinsic connectivity networks for salience processing and executive control. *J. Neurosci.* 27 (9), 2349–2356. <https://doi.org/10.1523/jneurosci.5587-06.2007>.
- Shaw, S.B., McKinnon, M.C., Heisz, J., Becker, S., 2021. Dynamic task-linked switching between brain networks - a tri-network perspective. *Brain Cogn.* 151, 105725. <https://doi.org/10.1016/j.bandc.2021.105725>.
- Shen, Y., Yao, J., Jiang, X., Zhang, L., Xu, L., Feng, R., Chen, W., 2015. Sub-hubs of baseline functional brain networks are related to early improvement following two-week pharmacological therapy for major depressive disorder. *Hum. Brain Mapp.* 36 (8), 2915–2927. <https://doi.org/10.1002/hbm.22817>.
- Smitha, K.A., Akhil Raja, K., Arun, K.M., Rajesh, P.G., Thomas, B., Kapilamoorthy, T.R., Kesavadas, C., 2017. Resting state fMRI: a review on methods in resting state connectivity analysis and resting state networks. *Neuroradiol. J.* 30 (4), 305–317. <https://doi.org/10.1177/1971400917697342>.
- Vaughn, K.A., DeMaster, D., Kook, J.H., Vannucci, M., Ewing-Cobbs, L., 2022. Effective connectivity in the default mode network after pediatric traumatic brain injury. *Eur. J. Neurosci.* 55 (1), 318–336. <https://doi.org/10.1111/ejn.15546>.
- Vincent, J.L., Snyder, A.Z., Fox, M.D., Shannon, B.J., Andrews, J.R., Raichle, M.E., Buckner, R.L., 2006. Coherent spontaneous activity identifies a hippocampal-parietal memory network. *J. Neurophysiol.* 96 (6), 3517–3531. <https://doi.org/10.1152/jn.00048.2006>.
- Wang, L., Hermens, D.F., Hickie, I.B., Lagopoulos, J., 2012. A systematic review of resting-state functional-MRI studies in major depression. *J. Affect. Disord.* 142 (1–3), 6–12. <https://doi.org/10.1016/j.jad.2012.04.013>.
- Warden, D., Rush, A.J., Trivedi, M.H., Fava, M., Wisniewski, S.R., 2007. The STAR*D Project results: a comprehensive review of findings. *Curr. Psychiatry Rep.* 9 (6), 449–459. <https://doi.org/10.1007/s11920-007-0061-3>.
- Whiteford, H.A., Degenhardt, L., Rehm, J., Baxter, A.J., Ferrari, A.J., Erskine, H.E., Vos, T., 2013. Global burden of disease attributable to mental and substance use disorders: findings from the Global Burden of Disease Study 2010. *Lancet* 382 (9904), 1575–1586. [https://doi.org/10.1016/s0140-6736\(13\)61611-6](https://doi.org/10.1016/s0140-6736(13)61611-6).
- Zheng, H., Xu, L., Xie, F., Guo, X., Zhang, J., Yao, L., Wu, X., 2015. The altered triple networks interaction in depression under resting state based on graph theory. *Biomed. Res. Int.* 2015. <https://doi.org/10.1016/j.jad.2016.09.005>.
- Zhong, X., Pu, W., Yao, S., 2016. Functional alterations of fronto-limbic circuit and default mode network systems in first-episode, drug-naïve patients with major depressive disorder: a meta-analysis of resting-state fMRI data. *J. Affect. Disord.* 206, 280–286. <https://doi.org/10.1155/2015/386326>.
- Zhu, X., Wang, X., Xiao, J., Liao, J., Zhong, M., Wang, W., Yao, S., 2012. Evidence of a dissociation pattern in resting-state default mode network connectivity in first-episode, treatment-naïve major depression patients. *Biol. Psychiatry* 71 (7), 611–617. <https://doi.org/10.1016/j.biopsych.2011.10.035>.